

Current in wave-driven plasmas

Charles F. F. Karney and Nathaniel J. Fisch

Plasma Physics Laboratory, Princeton University, Princeton, New Jersey 08544-0451

(Received 13 May 1985; accepted 11 October 1985)

A theory for the generation of current in a toroidal plasma by radio-frequency waves is presented. The effect of an opposing electric field is included, allowing the case of time varying currents to be studied. The key quantities that characterize this regime are identified and numerically calculated. Circuit equations suitable for use in ray-tracing and transport codes are given.

I. INTRODUCTION

In recent years there has been considerable interest in generating steady-state currents in a plasma with rf waves. In particular, it was predicted¹ that these currents could be efficiently generated by waves having phase velocities several times the electron thermal speed. This prediction has been confirmed by numerous experiments in which the current was driven by lower-hybrid waves. These results allow us to contemplate a steady-state tokamak reactor in which the toroidal current is driven by lower-hybrid waves. This is an attractive proposition not only because of the advantages inherent in steady-state operation (less thermal stress, higher duty cycle, etc.), but also because it opens up the possibility that the Ohmic winding of the tokamak can be eliminated entirely, leading to a cheaper and more compact reactor. This latter possibility can be realized if rf waves are successful not only in sustaining the plasma current "steady-state current drive," but also in increasing the plasma current "rf current ramp-up." In fact, experiments have demonstrated that this, too, is possible. From a theoretical point of view, the important additional ingredient in these experiments is the dc electric field, which opposes the increase of the plasma current. The electric field is also present in schemes where the rf is used to recharge the transformer at constant current.

Recently, we presented a theory for rf current drive in the presence of an electric field.² This theory predicted that rf energy could be efficiently converted to poloidal field energy if the wave phase velocity were approximately equal to the electron runaway velocity. This theory has been compared³ with data from the Princeton Large Torus (PLT) experiment,⁴ and excellent agreement is found. In Ref. 2 the linearized Boltzmann equation was approximately solved by integrating the corresponding Langevin equations using a Monte Carlo method. In this paper we use a more elegant theory to calculate the efficiency of the current ramp-up based on an adjoint formulation for the Boltzmann equation.⁵ Although the limits of validity of this theory are the same as for Ref. 2, this theory is more amenable to accurate evaluation on a computer, and it is more easily extended to include effects that are omitted here.

Let us begin by reiterating the physical picture given in Ref. 2. Consider an electron traveling in the positive direction at several times the thermal speed and which has just absorbed an incremental amount of rf energy. Suppose there is an electric field tending to decelerate this electron. The question is: Where does this incremental energy end up? If

the electron is slow compared to the runaway velocity, the electron slows down primarily because of collisions and so the rf energy goes to bulk heating. On the other hand, if the electron is fast, the electron is slowed down by the electric field. In this case the rf energy is coupled to the plasma circuit and appears as poloidal field energy. Unfortunately, fast electrons have a high probability of pitch-angle scattering into the reverse direction and running away. A runaway electron drains energy out of the electric field, leading to a degradation of the ramp-up efficiency. However, there is a window around the runaway velocity where the electrons are slowed down principally by the electric field and yet where the probability of running away is very small. This is the favorable regime in which rf energy can be efficiently converted to poloidal field energy.

From the foregoing discussion we see that two ingredients are needed for an accurate theoretical treatment of this problem. First, the electric field must be treated as large. In the efficient regime the force on the electron caused by the electric field must be comparable to that caused by collisions. Second, a two-dimensional treatment is required. Analyses based on a one-dimensional Fokker-Planck equation do not predict the important physical phenomenon of rf-generated reverse runaways.

We briefly review the history of theoretical studies of current drive in the presence of an electric field. The earliest theoretical studies¹ of lower-hybrid current drive assumed that there was no electric field in the plasma. This is the appropriate limit for a steady-state reactor. However, some of the early experiments conducted to verify the predictions of the theory were conducted in regimes where the Ohmic electric field was still present. This prompted a series of papers⁶⁻¹⁰ dealing with rf current drive in the presence of an assisting electric field (i.e., the electric field and the rf both accelerate the electrons in the same direction). The principal focus of these papers was the calculation of an enhanced runaway rate when the phase velocity of the waves is in the neighborhood of the runaway velocity. An opposing electric field was treated by Borrass and Nocentini¹¹ within the framework of a one-dimensional Fokker-Planck analysis. A similar model has been employed more recently by Liu *et al.*¹² As noted above, such an analysis cannot include rf-generated reverse runaways. Also, because of the crudity of the one-dimensional equation, the results are only accurate to within a factor of order unity even when no runaways are generated. A two-dimensional treatment of the problem in

the small electric field limit has been given by Start¹³ for the case of current drive by electron-cyclotron waves. This work neglected electron-electron collisions. This defect was removed and the results generalized to arbitrary current-drive methods by Fisch¹⁴ employing an adjoint formulation. This work yields accurate results when the electric field is small. However, the results are inapplicable in the regime of efficient ramp-up where the phase velocity is comparable to the runaway velocity. Our earlier paper² was the first to combine a two-dimensional treatment with a large electric field. This paper allowed an accurate calculation of the ramp-up efficiency in cases of practical interest, and identified the regime in which high efficiencies can be expected. The present work is a continuation and expansion of that earlier paper. Besides using the more sophisticated method⁵ for solving the Boltzmann equation, we endeavor to give the results in a form that allows both easy comparison with experiments and easy implementation within the framework of ray-tracing or transport codes.

The paper is organized as follows. We begin with the linearized Boltzmann equation for the perturbed electron distribution in the presence of an electric field and an rf source (Sec. II). Some approximations and normalizations are made to reduce this equation to a more manageable form. The use of the adjoint method⁵ for solving the resulting equation is described (Sec. III). Next (Sec. IV) the adjoint equation is solved numerically to give the runaway probability and the Green's function for the current. The latter quantity is reduced to a simple form that involves just two functions of velocity. An expression for the total current density is given (Sec. V), and this is put into a form that is easy to calculate. How the rf-driven current interacts with the electric field to produce poloidal field energy is considered (Sec. VI), and the results are applied to experiments.

II. BOLTZMANN EQUATION

Consider a uniform electron-ion plasma, initially at equilibrium. For $t > 0$, it is subject to an electric field $\mathbf{E}(t)$ and a wave-induced flux $\mathbf{S}(\mathbf{v}, t)$. We will take the ions to be infinitely massive, so that they form a stationary background off which the electrons collide. If the electric field and the wave-induced flux are weak enough, the electron distribution remains close to a Maxwellian for $\mathcal{E} \lesssim T$, where \mathcal{E} is the energy of an electron $\frac{1}{2}mv^2$. Substituting $f = f_m + f_1$ into the Boltzmann equation for the electron distribution f and linearizing then gives

$$\begin{aligned} \frac{\partial}{\partial t} f_1 + \frac{q\mathbf{E}(t)}{m} \cdot \frac{\partial}{\partial \mathbf{v}} f_1 - C(f_1) \\ = -\frac{\partial}{\partial \mathbf{v}} \cdot \mathbf{S} - \frac{q\mathbf{E}(t)}{m} \cdot \frac{\partial}{\partial \mathbf{v}} f_m \\ - \left[\frac{\dot{n}}{n} + \left(\frac{\mathcal{E}}{T} - \frac{3}{2} \right) \frac{\dot{T}}{T} \right] f_m, \end{aligned} \quad (1)$$

where

$$f_m = n(m/2\pi T)^{3/2} \exp(-\mathcal{E}/T)$$

and

$$C(f) = C(f, f_m) + C(f_m, f) + C(f, f_1)$$

is the linearized collision operator. Here q , m , n , and T are the electron charge, mass, number density, and temperature. Note that q carries the sign of the electron charge (i.e., $q = -e$).

This equation is to be solved with initial condition $f_1(\mathbf{v}, t = 0) = 0$. We demand that the subsequent evolution of f_1 be such that it be orthogonal to 1 and \mathcal{E} , i.e., that it have zero density and energy. The zero-density condition is satisfied with $\dot{n} = 0$ since all the terms in Eq. (1) are particle conserving. The zero-energy condition gives an equation for the time evolution of T :

$$\frac{3}{2} n \frac{dT}{dt} = \int m \mathbf{S} \cdot \mathbf{v} d^3\mathbf{v} + \mathbf{E} \cdot \int q \mathbf{v} f_1 d^3\mathbf{v}.$$

The two terms on the right-hand side represent the heating resulting from the waves and $\mathbf{E} \cdot \mathbf{J}$.

We now make three simplifying assumptions: we assume that f_1 is azimuthally symmetric about the ambient magnetic field; we take the electric field to be constant and in the direction parallel to the magnetic field $\mathbf{E} = E\hat{\mathbf{v}}_{\parallel}$; and we restrict our attention to those cases where \mathbf{S} is only finite where $v \gg v_r$, with $v_r^2 = T/m$ the thermal velocity. We may then solve Eq. (1) using the high-velocity form for C :

$$C(f) = \Gamma \left(\frac{1}{v^2} \frac{\partial}{\partial v} f + \frac{1+Z}{2v^3} \frac{\partial}{\partial \mu} (1-\mu^2) \frac{\partial}{\partial \mu} f \right),$$

where $\mu = v_{\parallel}/v$, $\Gamma = nq^4 \ln \Lambda / 4\pi\epsilon_0^2 m^2$, ϵ_0 is the dielectric constant of free space, $\ln \Lambda$ is the Coulomb logarithm, and Z is the effective ion charge state. We have included pitch-angle scattering and frictional slowing down, but ignored energy diffusion. In the problem of steady-state current drive,¹⁵ the energy diffusion term introduces corrections of order $(v_r/v)^2$. Another term neglected in this approximate collision operator is the effect of the Maxwellian colliding off the perturbed distribution $C(f_m, f)$. The corrections resulting from this term¹⁵ are of order $(v_r/v)^3$. With these approximations the collision operator does not depend on the electron temperature T . Formally, we may derive the form for C by taking $T \rightarrow 0$. In this limit we have $f_m \rightarrow n\delta(\mathbf{v})$.

It is convenient to introduce some normalizations. The runaway velocity v_r is that velocity at which collisional frictional force equals the acceleration caused by the electric field:

$$v_r \equiv -\text{sign}(qE) \sqrt{m\Gamma/|qE|}.$$

Notice that the sign of v_r is opposite to the direction in which electrons run away. The Dreicer velocity¹⁶ is given by $-\sqrt{2+Z}v_r$. Similarly, we define a runaway collision frequency

$$\nu_r \equiv \Gamma/|v_r|^3.$$

The normalized time and velocity are given by

$$\tau = \nu_r t$$

and

$$\mathbf{u} = \mathbf{v}/v_r.$$

The components of \mathbf{v} have to be normalized with care: $u_{\perp} = v_{\perp}/|v_r|$, $u_{\parallel} = v_{\parallel}/v_r$, and $u = v/|v_r|$. This implies that $u_{\parallel}/u = \text{sign}(v_r)v_{\parallel}/v$ so that the conversion of the pitch-angle variable μ in \mathbf{v} space to that in \mathbf{u} space involves multipli-

cation by $\text{sign}(v_r)$. Other quantities are normalized in a similar way; however, we shall use the same symbols as for the unnormalized quantities. Thus the distribution functions f_1 and f_m are normalized to $n/|v_r|^3$, the rf-induced flux \mathbf{S} to $nv_r v_r/|v_r|^3$, etc. Under this normalization, Eq. (1) then becomes

$$\frac{\partial}{\partial \tau} f_1 + D(f_1) = -\frac{\partial}{\partial \mathbf{u}} \cdot \mathbf{S}, \quad (2)$$

with $f_1(\mathbf{u}, \tau = 0) = 0$ and the operator D defined by

$$D \equiv -\frac{\partial}{\partial u_{\parallel}} - \frac{1}{u^2} \frac{\partial}{\partial u} - \frac{1+Z}{2u^3} \frac{\partial}{\partial \mu} (1-\mu^2) \frac{\partial}{\partial \mu}.$$

Equation (2) is singular at the origin. However, because f_1 in Eq. (2) describes a physical particle distribution, it obeys a particle conservation law near the origin. We therefore require that, close to $u = 0$, $f_1(\mathbf{u}) = N(\tau)\delta(\mathbf{u})$ with $N(0) = 0$ and

$$\frac{dN}{d\tau} = \lim_{u \rightarrow 0} \int_{-1}^1 2\pi f_1(u, \mu) d\mu.$$

Equation (2) depends only on a single parameter Z . The dependence on the electric field E can be normalized away, since the electric field defines the only natural velocity scale in the problem v_r .

Equation (2) is amenable to various methods of solution, and it is instructive to review these before describing the method used here. The most straightforward approach is to integrate Eq. (2) directly on a computer. This method allows \mathbf{S} to be determined directly in terms of the electron distribution f . However, a thorough understanding of the problem requires that many different forms of \mathbf{S} be used. Therefore this procedure is costly because the several parameters used to specify \mathbf{S} must be scanned. This is essentially the method adopted in the early numerical studies of steady-state current drive by lower-hybrid waves.¹⁷

The situation is improved to some extent by noting that Eq. (2) is a linear equation for f_1 . It may be solved in terms of a Green's function g given by the equation

$$\left(\frac{\partial}{\partial \tau} + D \right) g(\mathbf{u}, \tau; \mathbf{u}') = 0, \quad (3)$$

with $g(\mathbf{u}, \tau = 0; \mathbf{u}') = \delta(\mathbf{u} - \mathbf{u}')$. The electron distribution is then given by the convolution

$$f_1(\mathbf{u}, \tau) = \int_0^{\tau} d\tau' \int d^3\mathbf{u}' \mathbf{S}(\mathbf{u}', \tau') \cdot \frac{\partial}{\partial \mathbf{u}} g(\mathbf{u}, \tau - \tau'; \mathbf{u}').$$

This approach reduces the problem to the determination of a single function g of two vector arguments (\mathbf{u} and \mathbf{u}') and one scalar argument (τ). However, this is still a daunting computational task.

A closely related technique is to formulate the problem as a set of Langevin equations,¹⁸

$$\frac{du}{d\tau} = -\frac{1}{u^2} - \mu, \quad (4)$$

$$\frac{d\mu}{d\tau} = A(\tau) - \frac{1-\mu^2}{u},$$

where the pitch-angle scattering is represented by the stochastic term $A(\tau)$. Assuming that $u(\tau) = u$ and $\mu(\tau) = \mu$ are given (i.e., nonstochastic), then $A(\tau)$ satisfies

$$\langle A(\tau) \rangle = -[(1+Z)/u^3]\mu, \quad (5)$$

$$\langle A(\tau) A(\tau') \rangle = [(1+Z)/u^3](1-\mu^2)\delta(\tau - \tau'),$$

where the angle brackets denote averaging over the ensemble defined by all the realizations of A . Consider following a particular electron using Eqs. (4). Suppose that the electron is observed to travel with velocity \mathbf{u}' at $\tau = 0$. Then $g(\mathbf{u}, \tau; \mathbf{u}')d^3\mathbf{u}$ is the probability that the velocity of the electron at time τ is in the volume element $d^3\mathbf{u}$ located at \mathbf{u} . In Appendix A it is shown that this conditional probability g satisfies Eq. (3). Thus the solution to Eq. (3) can be found by determining the distribution of a large number of electrons obeying Eqs. (4) with initial conditions with $\mathbf{u}(\tau = 0) = \mathbf{u}'$. Consequently, moments of g can be determined by ensemble averages of the Langevin variables. For example, the current given by Eq. (3) may be found by

$$\int d^3\mathbf{u} u\mu g(u, \mu, \tau; u', \mu') = \langle u(\tau)\mu(\tau) \rangle.$$

Equations (4) may be integrated numerically by noting that

$$\int_{\tau}^{\tau + \Delta\tau} A(\tau') d\tau'$$

should be picked from an ensemble with mean $-(1+Z)\mu\Delta\tau/u^3$ and variance $(1+Z)(1-\mu^2)\Delta\tau/u^3$, where u and μ are the values of those variables at time τ . As long as $\Delta\tau$ is sufficiently small, further details about the distribution of A are unimportant.

Now Eqs. (4) are the equations solved in our earlier paper.² This shows the exact equivalence between the approach adopted there and that employed in the present work. Because the Langevin equations describe the electron behavior in a slightly more physical manner, they often help in the interpretation of the solutions to the Boltzmann equation. This is especially true when some electrons run away. The Langevin equations are also very easy to solve numerically by a Monte Carlo method (as was done in Ref. 2), although their solution tends to be much more costly than just solving Eq. (3) directly.

Equations (4), however, may be easily solved analytically in the limit $u \rightarrow 0$ (this is equivalent to taking the limit $E \rightarrow 0$). Taking an ensemble average of the equations, we obtain

$$\frac{du}{d\tau} = -\frac{1}{u^2}, \quad \frac{d\langle \mu \rangle}{d\tau} = -\frac{1+Z}{u^3} \langle \mu \rangle.$$

Note that u is not a stochastic variable in this limit. Consequently, the hierarchy of moment equations may be closed at this point. These are the slowing-down equations solved by Fisch and Boozer¹⁹ to give the current moment of electron distribution $\langle u\mu \rangle = u\langle \mu \rangle$. This shows that the approach used in that paper is equivalent to solving the Boltzmann equation.

III. ADJOINT METHOD

The methods for solving the Boltzmann equation described in the previous section all entail a large amount of computation. (An exception is the limit $E \rightarrow 0$, when the

ensemble-averaged Langevin equations can be solved analytically.¹⁹ The problem with these methods is that they are all capable of giving the electron distribution function f_1 . Since, in many cases, we are only interested in specific moments of f_1 , we may hope to reduce the computational requirements substantially by using a method that gives only those specific moments. Suppose we wish to determine a particular moment of f_1 , namely,

$$H(\tau) = \int d^3\mathbf{u} h_0(\mathbf{u}) f_1(\mathbf{u}, \tau).$$

[For instance, the current density would be given by $h_0(\mathbf{u}) = u_{\parallel}$.] Let us define the corresponding moment of the Green's function:

$$h(\mathbf{u}', \tau) = \int d^3\mathbf{u} h_0(\mathbf{u}) g(\mathbf{u}, \tau; \mathbf{u}'). \quad (6)$$

The moment H is then given in terms of h by

$$H(\tau) = \int_0^{\tau} d\tau' \int d^3\mathbf{u} \mathbf{S}(\mathbf{u}, \tau') \cdot \frac{\partial}{\partial \mathbf{u}} h(\mathbf{u}, \tau - \tau'). \quad (7)$$

What is needed is some method of calculating h that does not involve finding g . This is provided by the adjoint formulation of Fisch.⁵ He shows that $h(\mathbf{u}, \tau)$ satisfies

$$\frac{\partial}{\partial \tau} h + D^*(h) = 0, \quad (8)$$

with $h(\mathbf{u}, \tau = 0) = h_0(\mathbf{u})$ and the operator D^* defined by

$$D^* \equiv \frac{\partial}{\partial u_{\parallel}} + \frac{1}{u^2} \frac{\partial}{\partial u} - \frac{1 + Z}{2u^3} \frac{\partial}{\partial \mu} (1 - \mu^2) \frac{\partial}{\partial \mu}.$$

The singularity at the origin is handled by the boundary condition $h(\mathbf{u} = 0, \tau) = 0$. The operators D and D^* are adjoint operators, so that

$$\int (hD(f) - fD^*(h)) d^3\mathbf{u} = 0$$

for all $f(\mathbf{u})$ and $h(\mathbf{u})$ satisfying $f(\mathbf{u} \rightarrow \infty) = 0$ and $h(\mathbf{u} = 0) = 0$.

Similar techniques were introduced earlier by Antonsen and Chu²⁰ and by Taguchi²¹ for the study of steady-state current drive. The significant improvements afforded by Ref. 5 are the ability to determine arbitrary moments of f_1 and the inclusion of the time dependence of f_1 . Both of these are important in the problem of current ramp-up.

From the relation between the two Green's functions h and g , we see that h has a simple interpretation. Equations (3) and (4) describe the evolution of a group of electrons released at $\tau = 0$ at velocity \mathbf{u}' . Let us suppose that we are interested in the current density so that $h_0(\mathbf{u}) = u_{\parallel}$. Then $h(\mathbf{u}', \tau)$ gives the mean current carried by those electrons at time τ later. How Eq. (8) works is easily seen by taking $u \gg 1$ so that the electron only experiences the electric field. In the Boltzmann equation the electrons have slowed down to $\mathbf{u}' - \tau \hat{\mathbf{u}}_{\parallel}$ at time τ . Correspondingly in the adjoint equation, the initial condition h_0 is transported in the reverse direction so that $h(\mathbf{u}', \tau) = h_0(\mathbf{u}' - \tau \hat{\mathbf{u}}_{\parallel})$. Thus at time τ we are provided with information about the electrons in their current location.

Solving the Boltzmann equation by means of the adjoint formulation results in a great simplification of the problem. The adjoint equation (8) is an equation of equal complexity to

the original Boltzmann equation (2). However, by solving Eq. (8) for a particular initial condition, we can find the corresponding moment of f_1 using Eq. (7) for any driving term S .

The proof that h is given by Eq. (8) is most easily carried out by assuming that Eq. (8) holds and then by proving that h is related to the general Green's function g by Eq. (6). Consider the equation for $g(\mathbf{u}, \tau'; \mathbf{u}')$,

$$\left(\frac{\partial}{\partial \tau'} + D \right) g(\mathbf{u}, \tau'; \mathbf{u}') = 0.$$

We multiply this equation by $h(\mathbf{u}, \tau - \tau')$, integrate over all velocity space, and use the adjoint relation between D and D^* to give

$$\int d^3\mathbf{u} h(\mathbf{u}, \tau - \tau') \frac{\partial}{\partial \tau'} g(\mathbf{u}, \tau'; \mathbf{u}') + g(\mathbf{u}, \tau'; \mathbf{u}') D^*(h(\mathbf{u}, \tau - \tau')) = 0.$$

Substituting from Eq. (8) and integrating in τ' from 0 to τ gives

$$\int d^3\mathbf{u} h(\mathbf{u}, \tau - \tau') g(\mathbf{u}, \tau'; \mathbf{u}') \Big|_{\tau'=0}^{\tau} = 0.$$

If we evaluate this expression using the initial conditions for g and h , we obtain Eq. (6).

Up until now we have assumed that all the equations are solved in an infinite velocity domain. This is not a convenient formulation for numerical implementation where, necessarily, we wish to solve equations in a finite domain. Here we shall solve Eq. (8) only in a spherical domain V such that $u < u_b$. We will choose u_b to be sufficiently large that the interesting physics where the electric field competes with the collisions happens inside V . Outside V collisions may be ignored and the electrons are merely freely accelerated by the electric field. We must impose boundary conditions on Σ , the boundary of V . Again we follow the treatment given in Ref. 5. We begin by noting that both Eq. (2) and Eq. (8) are hyperbolic in the u direction. The boundary therefore divides into two pieces, depending on whether the characteristics enter or leave the domain. We define Σ_{in} (resp. Σ_{out}) as that portion of Σ on which $-\mu - 1/v^2 < 0$ (resp. > 0). The characteristics of Eq. (2) enter V on Σ_{in} and leave on Σ_{out} , while those of Eq. (8) enter V on Σ_{out} and leave on Σ_{in} . Boundary conditions must be specified where the characteristics enter the domain V . For u_b sufficiently large, the solution beyond Σ may be determined by ignoring collisions. Thus

$$f_1(\mathbf{u}, \tau) = f_1(\mathbf{u} + \tau \hat{\mathbf{u}}_{\parallel}, 0) = 0$$

for \mathbf{u} on Σ_{in} and

$$h(\mathbf{u}, \tau) = h(\mathbf{u} - \tau \hat{\mathbf{u}}_{\parallel}, 0) = h_0(\mathbf{u} - \tau \hat{\mathbf{u}}_{\parallel})$$

for \mathbf{u} on Σ_{out} . (If energy scattering had been included in the collision operator, the equations would revert to parabolic, and boundary conditions would have to be specified over the whole of Σ . However, there would be a boundary layer where the characteristics of the approximate equations are outgoing, and the boundary conditions here would only weakly affect the solution in the interior of V .)

Although Eq. (8) was derived under the simplifying assumptions that the electric field was constant and the high-

velocity form of collision operator is valid, the adjoint method as described in Ref. 5 applies equally well without such restrictive assumptions. Thus the equation adjoint to Eq. (1) reads⁵

$$\left(\frac{\partial}{\partial t'} - \frac{q\mathbf{E}(t-t')}{m} \cdot \frac{\partial}{\partial \mathbf{v}} - C^*\right)h(\mathbf{v}, t'; t) = q_1 + q_2 \mathcal{E}, \quad (9)$$

where C^* is the operator adjoint to C . Since the full linearized collision operator is self-adjoint, we have $C^*(h) = C(f_m h)/f_m$. Equation (9) is to be solved with the initial condition $h(\mathbf{v}, t' = 0; t) = h_0(\mathbf{v})$. We restrict $f_m h$ to being orthogonal to 1 and \mathcal{E} and q_1 and q_2 are chosen to ensure that this condition on $f_m h$ remains satisfied given that it is satisfied initially. It can then be shown⁵ that

$$\int d^3\mathbf{v} f_1(\mathbf{v}, t) h_0(\mathbf{v}) = \int_0^t dt' \int d^3\mathbf{v} \mathbf{S}_*(\mathbf{v}, t') \cdot \frac{\partial}{\partial \mathbf{v}} h(\mathbf{v}, t-t'; t), \quad (10)$$

where $\mathbf{S}_*(\mathbf{v}, t) = \mathbf{S}(\mathbf{v}, t) + [q\mathbf{E}(t)/m] f_m$. This equation will enable us to incorporate the effects of a slowly varying electric field into our analysis. It also makes explicit the additive nature of those effects caused by the electric field alone (i.e., with $\mathbf{S}_* = \mathbf{S}$). Of course, the effects caused by the electric field alone are well studied and give rise to phenomena such as the Spitzer-Härm conductivity²² and runaways.¹⁶

IV. SOLUTIONS TO THE ADJOINT EQUATION

Moments of the electron distribution f_1 can now be calculated by solving Eq. (8) with the corresponding initial and boundary conditions. In practice this procedure still offers us too much information. Both for a deeper understanding of the underlying physics and for easy implementation in numerical codes, the trick is to discover the few important functions by which the major effects can be described. In this section we determine those functions needed for an accurate treatment of rf current ramp-up.

Let us suppose that rf flux is present only for some finite time. Electrons obeying Eq. (2) then eventually suffer one of two fates. Either they run away under the influence of the electric field $u_{\parallel} \rightarrow -\infty$, or else they collapse into the electron bulk $u \rightarrow 0$. We classify these two groups of electrons as "runaway" (subscript r) and "stopped" (subscript s), respectively. In a real plasma, i.e., $T \neq 0$, even the bulk particles will eventually run away. However, the time t_r it takes for these bulk electrons to run away is exponentially large, i.e., $\log t_r \sim (v_r/v_e)^2$. Our analysis is valid for times short compared with the bulk runaway time.

Runaways are very important in the calculation of the ramp-up efficiency because runaways gain energy at the expense of the poloidal magnetic field. Unless they are lost, even a small number of runaways can greatly reduce the ramp-up efficiency. Runaways may be defined as those particles with $u > u_0$ for $\tau \rightarrow \infty$, where u_0 is some arbitrary positive speed. (The number of runaways is independent of u_0 .) Therefore, their number is given by Eq. (7), with $\tau \rightarrow \infty$ and $h_0(\mathbf{u}) = 1$ for $u > u_0$ and 0 otherwise. The Green's function for the runaway number is given by $R(\mathbf{u})$

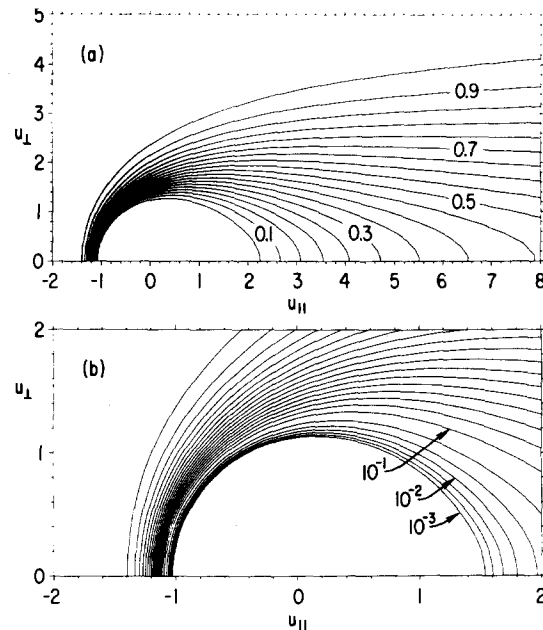


FIG. 1. The runaway probability $R(\mathbf{u})$ for $Z = 1$. Parts (a) and (b) show R on two different scales. In (a) the contours are equally spaced at intervals of 0.05. In (b) the seven lowest contours are geometrically spaced at intervals of $10^{1/3}$ between 10^{-3} and 10^{-1} ; the remaining contours are equally spaced at intervals of 0.05 as in (a).

$\equiv h(\mathbf{u}, \tau \rightarrow \infty)$, where R obeys

$$D^*(R(\mathbf{u})) = 0, \quad (11)$$

with boundary condition $R(\mathbf{u}) = 1$ on Σ_{out} . This function is the "runaway probability," the probability that an electron initially at \mathbf{u} runs away under the combined influence of the electric field and collisions.

Equation (11) was solved numerically with the boundary at $u_b = 10$. A term $\partial R / \partial \tau$ was included on the left-hand side, and the resulting equation was integrated until $\tau = 100$. A spherical ($u, \theta = \arccos \mu$) grid was used with a mesh size of 500×100 . The equation was integrated with an alternating direction implicit (ADI) scheme with a time step $\Delta\tau = 0.01$. The same method was used to solve the other equations given below.

In Fig. 1 we plot $R(\mathbf{u})$ for $Z = 1$. For $u < 1$, R is identically zero because the magnitude of the electrical force is less than that of the frictional force. One of the most important applications of these results is to drive current by lower-hybrid waves. In this case \mathbf{S} is in the parallel direction and is localized near $u_{\perp} = 0$. Therefore we need only know $R(u_{\parallel}, u_{\perp} = 0)$, which is plotted in Fig. 2 for $Z = 1, 2, 5$, and

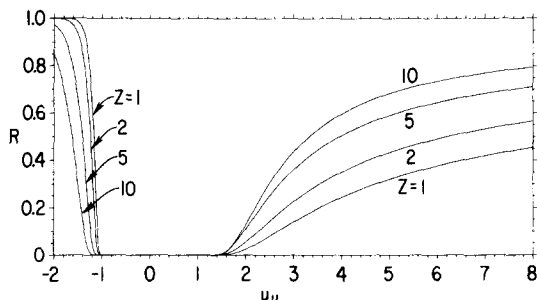


FIG. 2. The plot of $R(u_{\parallel}, u_{\perp} = 0)$ for $Z = 1, 2, 5$, and 10.

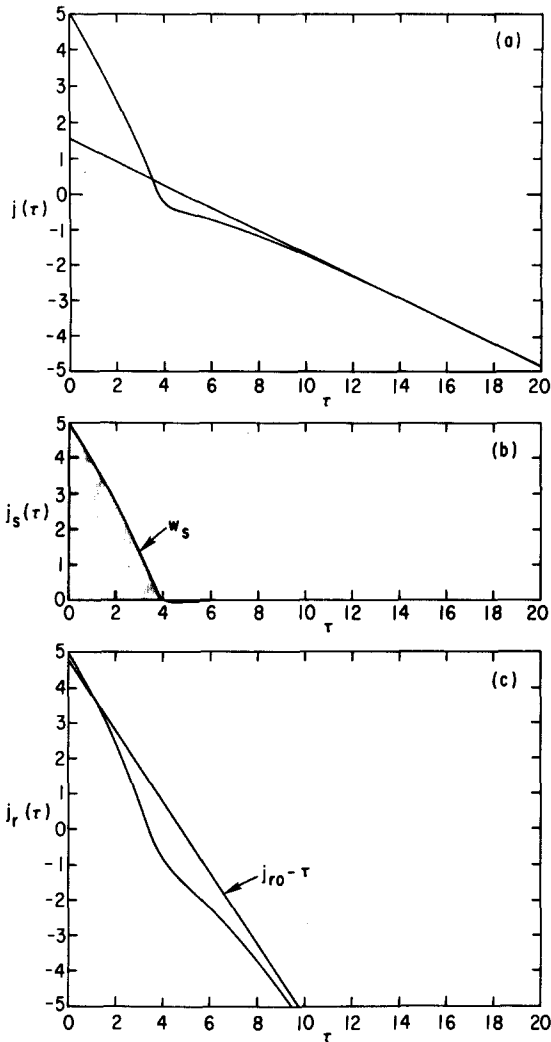


FIG. 3. The current $j(u, \tau)$ for $u = 5\hat{u}_{\parallel}$ and $Z = 1$; (a) the total current j ; (b) the stopped current j_s ; (c) the runaway current j_r . For $u = 5\hat{u}_{\parallel}$, approximately 32% of the electrons run away.

10. From this plot we see that we can effectively avoid the creation of runaways by operating with waves having phase velocities that lie in the range $0 < u_{\parallel} \lesssim 1.5$.

The next important quantity to determine is the current density carried by f_1 . This is given (in units of qnv_e) by Eq. (7) with $h_0(u) = u_{\parallel}$. The Green's function for the current $j(u, \tau)$ is therefore given by $\partial j / \partial \tau + D^*(j) = 0$ with initial condition $j(\tau = 0) = u_{\parallel}$ and boundary condition $j = u_{\parallel} - \tau$ on Σ_{out} . This is the mean current (in units of qv_e) carried by an electron initially at velocity u . In Fig. 3(a) we plot $j(u, \tau)$ as a function of τ for $u = 5\hat{u}_{\parallel}$ and $Z = 1$. Because the presence of runaways leads to a secular behavior ($j \sim \tau$) for large times, it is helpful to distinguish the current carried by stopped and runaway electrons. We write

$$j(u, \tau) = (1 - R(u))j_s(u, \tau) + R(u)j_r(u, \tau).$$

The quantity j_s (resp. j_r) is the mean current carried by an electron given that it eventually stops (resp. runs away). An electron at velocity u runs away with probability $R(u)$. Thus it contributes $(1 - R(u))u_{\parallel}$ to the stopped current and $R(u)u_{\parallel}$ to the runaway current. These quantities are therefore the initial conditions to the adjoint equations for $(1 - R)j_s$ and

Rj_r , respectively, so that

$$\left(\frac{\partial}{\partial \tau} + D^*\right)(1 - R)j_s = \left(\frac{\partial}{\partial \tau} + D^*\right)Rj_r = 0,$$

with $j_s(\tau = 0) = j_r(\tau = 0) = u_{\parallel}$ and $j_s = j_r = u_{\parallel} - \tau$ on Σ_{out} .

The stopped and runaway currents j_s and j_r are plotted in Figs. 3(b) and 3(c) for the same case as Fig. 3(a). Evidently j_s vanishes for $\tau \rightarrow \infty$ (since the electrons cease to carry any current once they are stopped). The time it takes for electrons to be stopped is of the order of u . Assuming that this time is short compared to the time scale for the variation of the rf flux S , we may replace $j_s(u, \tau)$ by $W_s(u)\delta(\tau)$, where $W_s(u) = \int_0^{\infty} j_s(u, \tau)d\tau$. The equation for W_s is obtained by integrating Eq. (8) over time to give

$$D^*[(1 - R(u))W_s(u)] = (1 - R(u))u_{\parallel}, \quad (12)$$

with $(1 - R)W_s = 0$ on Σ_{out} . Here W_s can be interpreted as the energy (in units of mv_e^2) imparted to the electric field by an electron as it slows down. In Fig. 4(a) we plot $W_s(u)$ for $Z = 1$. In the limit $u_{\parallel} \rightarrow \infty$, collisions are extremely weak, and all of the kinetic energy of the stopped particles goes into the electric field, i.e.,

$$W_s(u_{\parallel} \rightarrow \infty, u_{\perp} = 0) \rightarrow \frac{1}{2}u_{\parallel}^2.$$

In the limit $u \ll 1$, the electric field weakly perturbs the electron motion. Then, W_s is given by the theory of steady-state current drive,^{19,20} and corrections linear in the electric field are given by the hot conductivity.¹⁴ In our notation these results may be summarized by

$$W_s(u \ll 1, \mu) = \frac{\mu u^4}{5 + Z} - \frac{(2 + Z + 3\mu^2)u^6}{3(3 + Z)(5 + Z)}. \quad (13)$$

This function is plotted in Fig. 4(b). (An approximation to

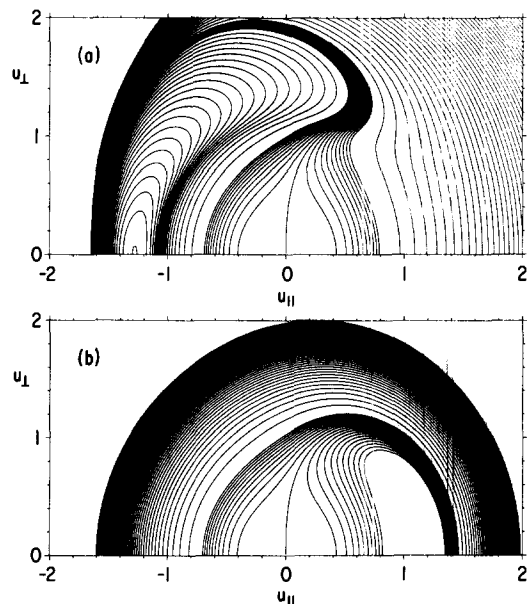


FIG. 4. The energy imparted to the electric field by the stopped particles $W_s(u)$ for $Z = 1$. The innermost contours are equally spaced at intervals of 0.005 between -0.05 and 0.05 . The remaining contours are equally spaced at intervals of 0.05. Part (a) shows the results of numerically solving Eq. (12); part (b) shows W_s from the hot-conductivity theory Eq. (13).

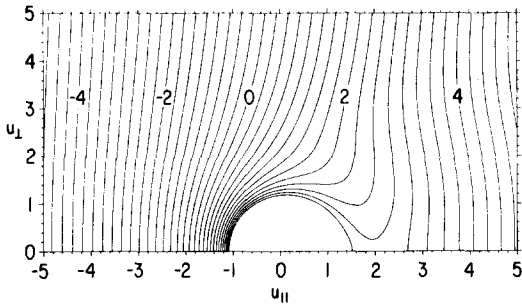


FIG. 5. The function $j_{r,0}(\mathbf{u})$ for $Z = 1$. The contours are equally spaced at intervals of 0.25.

W_s , correct to order u^{10} is given in Appendix B.) This linearized theory, however, is inapplicable for $u \sim 1$, and the behavior of this function is completely wrong for $u \gtrsim 1$.

Let us now turn to the contributions of the runaways to the current. The leading order contribution to j_r is $-\tau$. Let us therefore write

$$j_r(\mathbf{u}, \tau) = -\tau + j_{r,0}(\mathbf{u}) + j'_r(\mathbf{u}, \tau), \quad (14)$$

where $j'_r(\tau \rightarrow \infty) \sim 1/\tau$ and $j_{r,0}$ may be interpreted as the effective starting velocity for the runaways; see Fig. 3(c). The function $j_{r,0}$ is given by

$$D^*(R(\mathbf{u})j_{r,0}(\mathbf{u})) = R(\mathbf{u}),$$

with boundary condition $j_{r,0} = u_{||}$ on Σ_{out} . This function is shown in Fig. 5. For $u \gg 1$, the runaway electrons are only weakly perturbed by collisions so that $j_{r,0}(\mathbf{u}) \approx u_{||}$. Close to $u = 1$, collisions hold back the runaway electrons and $j_{r,0}(\mathbf{u})$ becomes large. However, it is not very important to know $j_{r,0}$ and j'_r very accurately since they are usually dominated by the first term in Eq. (14). We will approximate $j_{r,0}(\mathbf{u})$ by $u_{||}$ and will ignore $j'_r(\mathbf{u}, \tau)$ to give $j_r(\mathbf{u}, \tau) = u_{||} - \tau$.

Finally, we can write the Green's function for the current in an expedient form as

$$j(\mathbf{u}, \tau) = (1 - R(\mathbf{u})) W_s(\mathbf{u}) \delta(\tau) + R(\mathbf{u})(u_{||} - \tau). \quad (15)$$

In this form it depends only on two scalar functions of \mathbf{u} , namely, R and W_s . Approximate fits to these functions are given in Appendix B. An easy but important generalization is possible here and that is to allow a loss mechanism for runaways. This is done by modifying suitably the term $u_{||} - \tau$. For example, if the loss of runaways can be characterized by a loss time τ_{loss} , this term should be multiplied by $\exp(-\tau/\tau_{loss})$.

Using this formulation, many other moments of f_1 may be found. For example, we may wish to know the mean perpendicular energy of the runaway particles \mathcal{E}_{1r} (in units of mv_r^2) as they leave the integration region V . (The loss rate for runaways may depend on this quantity.) This is given by

$$D^*(R(\mathbf{u}) \mathcal{E}_{1r}(\mathbf{u})) = 0,$$

with $\mathcal{E}_{1r} = \frac{1}{2} u_{\perp}^2$ on Σ_{out} . (This result depends logarithmically on the value of u_b .) We have plotted this in Fig. 6. For electrons with $u_{||} > 1$ and $u_{\perp} = 0$, \mathcal{E}_{1r} is about 3. This reflects the necessity for the electrons to suffer appreciable pitch-angle scattering if they are to run away.

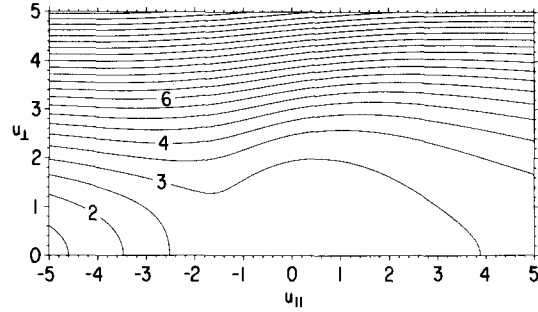


FIG. 6. The perpendicular energy of the runaways $\mathcal{E}_{1r}(\mathbf{u})$ for $Z = 1$. The contours are equally spaced at intervals of 0.5.

V. CIRCUIT EQUATIONS

When rf energy is injected into a tokamak, it induces a flux \mathbf{S} of electrons in velocity space. The power deposited per unit volume is then given by

$$p_{rf}(t) = \int d^3\mathbf{v} m \mathbf{S}(\mathbf{v}, t) \cdot \mathbf{v}. \quad (16)$$

Here p_{rf} , \mathbf{S} , and the other intensive physical quantities introduced in this section also depend on position \mathbf{r} . For brevity this dependence is not shown in the arguments to these quantities. This equation may be used in two ways. In detailed studies of rf current ramp-up based, for instance, on a ray-tracing model, we can estimate $\mathbf{S}(\mathbf{v}, t)$ on each flux surface by solving a one- or two-dimensional Fokker-Planck equation. Equation (16) then gives us the power deposition, p_{rf} . Alternatively, we can take the experimental measurements together with an energy balance of the rf energy to give us an estimate of p_{rf} . This, together with an approximate knowledge of where in velocity space the rf flux is localized, allows us to determine \mathbf{S} . In addition to causing power absorption, the flux \mathbf{S} leads to numerous other effects, such as rf-driven current, rf-enhanced particle transport, etc. Here our primary concern is with the rf-driven current. From Eq. (10) we see that this enters additively to the Ohmic current so that the total current density is given by the constitutive relation

$$\mathbf{J}(t) = \sigma(t) \mathbf{E}(t) + \mathbf{J}_{rf}(t), \quad (17)$$

where $\sigma(t)$ is the Spitzer-Härm conductivity²² for a Maxwellian plasma characterized by the background electron temperature $T(t)$ and \mathbf{J}_{rf} is the rf-driven current density. Here we have assumed that $|v_r| \gg v_r$, so that in the absence of any rf we can ignore runaways. Incorporation of this effect merely requires the addition of the current carried by the Dreicer runaway electrons in Eq. (17).

The rf-driven current density is given by Eq. (10) with the h placed by the current Green's function j and with $\mathbf{S}_* = \mathbf{S}$. Let us begin by writing j in unnormalized units. The form for j given in Eq. (15) will be sufficiently accurate for our purposes. Multiplying by qv_r gives

$$j(\mathbf{v}, t) = \frac{qv_r}{v_r} (1 - R(\mathbf{u})) W_s(\mathbf{u}) \delta(t) + qR(\mathbf{u}) \left(v_{||} + \frac{qE}{m} t \right),$$

where $\mathbf{u} = \mathbf{v}/v_r$. Here j is now a dimensional quantity, but W_s and R remain dimensionless functions of a dimensionless argument. In deriving this form for j we assumed that E and n were constant. We now relax this constraint, allowing

them both to vary on a time scale long compared to the runaway collision time ν_r^{-1} . (Recall that \mathbf{S} is also allowed to vary on the same time scale.) We can then write j as

$$j(\mathbf{v}, t - t'; t) = \frac{qv_r(t')}{\nu_r(t')} (1 - R(\mathbf{u}')) \mathcal{W}_s(\mathbf{u}') \delta(t - t') + qR(\mathbf{u}') \left(v_{\parallel} + \frac{q}{m} \int_{t'}^t E(s) ds \right), \quad (18)$$

where $\mathbf{u}' = \mathbf{v}/v_r(t')$. The additional parametric argument t here has the same meaning as in Eq. (9). In this form, $j(\mathbf{v}, t - t'; t)$ is the mean current carried by an electron at time t given that it was traveling at velocity \mathbf{v} at time t' . From Eq. (10) the rf-generated current density may now be written as

$$J_{\text{rf}}(t) = \int_0^t dt' \int d^3\mathbf{v} \mathbf{S}(\mathbf{v}, t') \cdot \frac{\partial}{\partial \mathbf{v}} j(\mathbf{v}, t - t'; t). \quad (19)$$

In order to write J_{rf} in a more useful form, we first define a runaway density n_r (in electrons per unit volume). This is given by

$$\frac{\partial n_r(t)}{\partial t} = \frac{1}{v_r(t)} \int d^3\mathbf{v} \mathbf{S}(\mathbf{v}, t) \cdot \frac{\partial}{\partial \mathbf{u}} R(\mathbf{u}), \quad (20)$$

with initial condition $n_r(t=0) = 0$. Substituting Eq. (18) into Eq. (19), we obtain

$$J_{\text{rf}}(t) = J_s(t) + J_r(t), \quad (21a)$$

where

$$J_s(t) = \frac{q}{v_r(t)} \int d^3\mathbf{v} \mathbf{S}(\mathbf{v}, t) \cdot \frac{\partial}{\partial \mathbf{u}} (1 - R(\mathbf{u})) \mathcal{W}_s(\mathbf{u}), \quad (21b)$$

$$\frac{\partial J_r(t)}{\partial t} = \frac{q^2}{m} E(t) n_r(t) + q \int d^3\mathbf{v} \mathbf{S}(\mathbf{v}, t) \cdot \frac{\partial}{\partial \mathbf{u}} R(\mathbf{u}) u_{\parallel}, \quad (21c)$$

with $J_r(t=0) = 0$. In Eqs. (20) and (21), \mathbf{u} is normalized in terms of the runaway velocity at time t , $\mathbf{u} = \mathbf{v}/v_r(t)$. These equations allow the current to be calculated by characterizing the runaway population with just two state variables n_r and J_r . Equations (16), (17), (20), and (21) suffice to give a detailed description of rf current ramp-up. In this form, Eq. (17) is suitable for substituting into a transport or ray-tracing code. Furthermore, it would be easy to modify Eq. (20) to include a loss mechanism for the runaways. Relativistic effects on the runaways could be included in an approximate fashion by limiting $|J_r(t)/qn_r(t)|$ to c , the speed of light. Such effects could be treated in a more systematic manner by modifying the term in large parentheses in Eq. (18) to read $v_{\parallel}(t)$, where

$$v_{\parallel}(t) = p_{\parallel}(t)/m\gamma,$$

$$p_{\parallel}(t) = mv_{\parallel} + \int_{t'}^t qE(s) ds,$$

$$\gamma = \sqrt{1 + p_{\parallel}^2(t)/m^2c^2}.$$

The resulting expression for $j(\mathbf{v}, t - t'; t)$ is valid for $v_r^2 \ll c^2$ and $v^2 \ll c^2$. Unfortunately, this is a significantly more cumbersome expression from which to calculate J_{rf} because, in order to determine the state of the plasma at a particular instant, the entire runaway distribution must be given (instead of just n_r and J_r).

VI. APPLICATIONS

The circuit equations written in Sec. V allow us to explore how J_{rf} interacts with the electric field to yield an efficient conversion of rf energy into poloidal magnetic field energy. It is helpful to convert to extensive physical quantities by assuming that the plasma current is carried in a channel of area A in which the plasma properties are approximately uniform. Thus, the total current is given by $I = AJ$, the total rf power deposited in the electrons by $P_{\text{in}} = 2\pi R_0 A p_{\text{rf}}$ (where R_0 is the tokamak major radius), the loop voltage by $V = 2\pi R_0 E$, etc. The plasma current is again written as the sum of Ohmic and rf contributions:

$$I = V/R_{\text{Sp}} + I_{\text{rf}}, \quad (22)$$

where $R_{\text{Sp}} = 2\pi R_0/A\sigma$ is the plasma (Spitzer-Härm) resistance. Faraday's law relates the rate of change of the current to the voltage,

$$V = -L\dot{I} + V_{\text{ext}}, \quad (23)$$

where L is the total plasma inductance, which for simplicity we shall take to be constant, V_{ext} is the voltage induced by the external coils (usually a combination of the Ohmic windings and the vertical field coils), and $\dot{I} \equiv dI/dt$. Multiplying this equation by I and substituting for I from Eq. (22) gives

$$\dot{W} = P_{\text{ext}} + P_{\text{el}} - V^2/R_{\text{Sp}}, \quad (24)$$

where $W \equiv \frac{1}{2}LI^2$ is the poloidal field energy, $P_{\text{ext}} \equiv V_{\text{ext}}I$ is the power coupled from the external circuits, and $P_{\text{el}} \equiv -VI_{\text{rf}}$ is the power coupled from the rf source into electromagnetic energy. This equation describes the energy balance for the poloidal magnetic field. The practical measure of the efficiency of current ramp-up is

$$\frac{\dot{W} - P_{\text{ext}}}{P_{\text{rf}}} = \frac{P_{\text{el}} - V^2/R_{\text{Sp}}}{P_{\text{rf}}}, \quad (25)$$

where P_{rf} is the total rf power injected into the plasma. The rf power absorbed by the electrons P_{in} is related to P_{rf} by $P_{\text{in}} = \eta P_{\text{rf}}$, where η is the absorption factor. The determination of η is beyond the scope of this paper; presumably it can be found by ray-tracing theories or by a power balance. The overall picture of the flow of power in an experiment is as follows. The rf power P_{rf} is injected into the machine. Of this a fraction η is absorbed by the resonant electrons; the rest may be absorbed by the ions or by the vacuum vessel. A fraction $P_{\text{el}}/P_{\text{in}}$ of this power is then converted into electromagnetic energy. Here P_{ext} acts as another source of poloidal field energy, while the Ohmic dissipation V^2/R_{Sp} acts as a drain. From this discussion we see that $P_{\text{el}}/P_{\text{in}}$ describes the "ideal" efficiency of rf current ramp-up. The practical efficiency is expressible in terms of this efficiency η and V^2/R_{Sp} .

The determination of $P_{\text{el}}/P_{\text{in}}$ from Eq. (21) is complicated by the presence of runaways. Runaways are deleterious to the ramp-up efficiency since their current is in the same direction as E and so they subtract from P_{el} . For efficient current ramp-up we must either avoid creating runaways by making sure \mathbf{S} is localized in that region of velocity space where the runaway probability R is small (see Figs. 1 and 2), or else take steps to lose the runaways. We can approximately treat these cases by taking $R = 0$ in Eq. (21) to give

$$\frac{P_{el}}{P_{in}} = \frac{\int d^3\mathbf{u} \mathbf{S} \cdot \partial W_s / \partial \mathbf{u}}{\int d^3\mathbf{u} \mathbf{S} \cdot \mathbf{u}}$$

Since this involves the ratio of two integrals over \mathbf{u} , the result is insensitive to the detailed form of \mathbf{S} . In cases of practical interest, we may assume that \mathbf{S} is localized in \mathbf{u} . Then, we have

$$\frac{P_{el}}{P_{in}} = \frac{\hat{\mathbf{S}} \cdot \partial W_s / \partial \mathbf{u}}{\hat{\mathbf{S}} \cdot \mathbf{u}}, \quad (26)$$

where \mathbf{u} is the normalized velocity of the resonant electrons.

For lower-hybrid waves we have $\hat{\mathbf{S}} = \hat{\mathbf{u}}_{\parallel}$ and the waves interact with particles through the Landau resonance $\omega - k_{\parallel} v_{\parallel} = 0$, where ω and k_{\parallel} are the wave frequency and parallel wave number. Furthermore, the typical perpendicular velocity of the resonant electrons equals the electron thermal velocity, so that $v_{\perp} \sim v_r \ll v_{\parallel}$. Thus Eq. (26) is to be evaluated with $u_{\parallel} = \omega/k_{\parallel} v_r$ and $u_{\perp} = 0$. This gives

$$\frac{P_{el}}{P_{in}} = \frac{\partial W_s / \partial u}{u}. \quad (27a)$$

This efficiency is plotted in Fig. 7(a). Approximate fits for this function are given in Appendix B.

On the other hand, for electron-cyclotron waves that interact through the Doppler-shifted cyclotron resonance $\omega - k_{\parallel} v_{\parallel} = l\Omega$, where Ω is the cyclotron frequency and l is the harmonic number, we have $\hat{\mathbf{S}} = \hat{\mathbf{u}}_{\perp}$. In this case we evaluate Eq. (26) at $u_{\parallel} = (\omega - l\Omega)/k_{\parallel} v_r$ and $u_{\perp} = 0$ to give

$$\frac{P_{el}}{P_{in}} = \frac{\partial W_s / \partial u - (1/u_{\parallel}) \partial W_s / \partial \mu}{u}, \quad (27b)$$

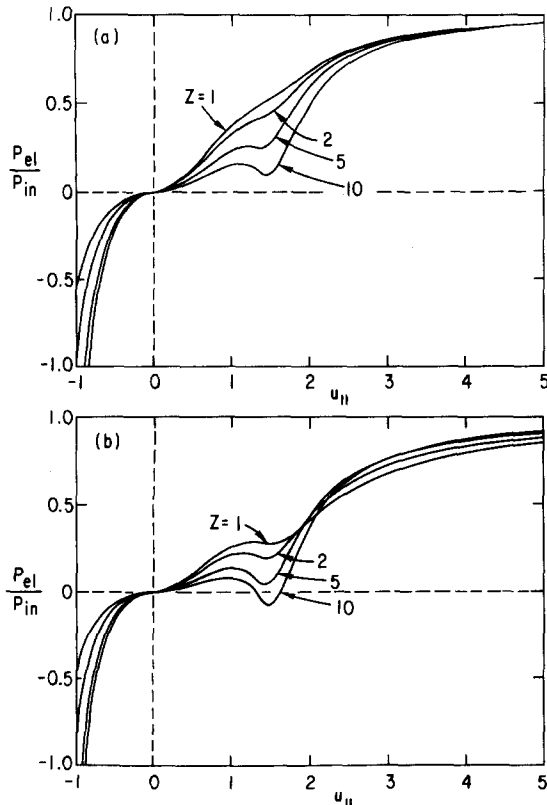


FIG. 7. Efficiency for lower-hybrid current drive (a) and for electron-cyclotron current drive (b) from Eqs. (27).

which is plotted in Fig. 7(b).

Using Eqs. (27) it is possible to identify regions of high conversion efficiency of wave energy to electric energy, given the restriction of R small. Additionally, if the Ohmic losses V^2/R_{sp} are small, then by Eq. (25) we see that the conversion of wave energy to poloidal field energy can be of high efficiency. This, in fact, is what has been achieved on the PLT experiment, where conversion efficiencies of over 25% have been reported.⁴

An important practical consequence of the circuit equations derived here is that fast ramp-up rates, i.e., large \dot{I} , are possible at high density. In fact, these fast ramp-up rates are *necessary* for high-energy conversion efficiencies at high density. This can be seen as follows. The efficiency P_{el}/P_{in} is a function of the dimensionless parameter u_{\parallel} , depending, in addition, only weakly on Z . For a given machine and a given wave phase velocity, the parameter u_{\parallel} depends only on the ratio E/n , and the ramp-up rate \dot{I} depends only on the dc electric field E . Thus the efficiency depends only on the ratio of \dot{I} to n . It has been observed experimentally on the PLT experiment that high efficiency of converting rf energy to magnetic field energy is possible at a low plasma density. Thus we can predict that a similar high efficiency is possible in the event that the density and the ramp-up rate are scaled up together. In fact, for large ramp-up rates, high density can actually be desirable in that it impedes the production of runaways. Note that this window of desired density for a given ramp-up rate is counter to our intuition derived from steady-state considerations, where the larger the density the less the current-drive efficiency.

There are several optimizations that one might wish to achieve in the ramp-up problem. One is to maximize the energy conversion efficiency P_{el}/P_{in} . A second is to minimize the ramp-up time $T_{ramp} \equiv I/\dot{I}$. The minimization of capital costs for the rf system, however, may demand that we minimize P_{rf} , the rf power required to ramp-up a given current.

We can express this more precisely with some convenient formulas. In the absence of the external source V_{ext} , the ramp-up rate may be written using Faraday's law as

$$\dot{I} \approx \frac{5E}{\ln R_0/a} \frac{\text{MA}}{\text{sec}}, \quad (28)$$

where a tokamak inductance $L \approx \mu_0 R_0 \ln R_0/a$ was assumed, and where E is the dc electric field in units of V/m. Note that the ramp-up rate depends linearly on E and is almost independent of geometry ($\ln R_0/a \approx 1$). The amount of dissipated rf power required can then be written as

$$P_{rf} \approx \frac{1}{\eta} \frac{1}{2} L I^2 \left(\frac{P_{el}}{P_{in}} \right)^{-1}, \quad (29)$$

if we neglect both ohmic losses (V^2/R_{sp}) and the external source P_{ext} . Thus, in extrapolating results to larger tokamaks (higher $\frac{1}{2} L I^2$), we can maintain linear (in the required stored energy) power requirements, with the same ramp-up time and the same efficiencies, if the density scales linearly with \dot{I} and hence with I . Here the wave phase velocities also remain the same, and in the event of the same temperatures, the physics of the damping may be expected to be very similar, so that the percentage of incident rf power that is absorbed, η , remains constant, too.

For example, in the PLT experiment with $n \approx 2 \times 10^{12} \text{ cm}^{-3}$, $T \approx 1 \text{ keV}$, $\omega/k_{\parallel} \approx 6v_i \approx \frac{1}{4}c$, we find reported ramp-up rates of $\dot{I} = 120 \text{ kA/sec}$, or $E \approx 24 \text{ mV/m}$. Here $u_{\parallel} \approx 1.4$, and ideal efficiencies of about 33% at $Z = 1$ may be expected with little runaway production, consistent with experimental data. Also a somewhat higher Z would be consistent with the data, but then only if the confinement of runaways were not perfect.

For reactor-grade tokamaks, say $LI^2 \approx 400 \text{ MJ}$ and $I \approx 10 \text{ MA}$, a ramp-up time longer than that in PLT is desirable in order to minimize P_{rf} and the capital cost of the rf system. For a 30 sec ramp-up time, a density of $5 \times 10^{12} \text{ cm}^{-3}$ renders the ratio \dot{I}/n as in the PLT experiment. Employing a similar spectrum of waves ($\omega/k_{\parallel} = \frac{1}{4}c$) in a plasma of temperature also similar to the PLT experiment ($T \approx 1 \text{ keV}$) implies a similar η (about 0.7). Thus using Eq. (29), we see that $P_{\text{rf}} \approx 40 \text{ MW}$ would be required.

To summarize the tradeoffs here, we note that while $P_{\text{el}}/P_{\text{in}}$ is minimized by considering only the ratio \dot{I}/n , the minimization of P_{rf} requires that T_{ramp} be large. Thus although very quick ramp-up rates are indeed achievable at high density, the capital costs for such a system are proportionately larger, too. Balancing the desires for a quick ramp-up against those for low capital costs (low P_{rf}) points to a parameter range of moderate density. Efficient ramp up is only achieved when, in addition to the above restrictions, the temperature is moderate, since at high temperatures, V^2/R_{sp} losses, neglected in Eq. (29), begin to dominate. The regime where these Ohmic losses dominate may be identified by writing

$$\frac{V^2}{R_{\text{sp}}} \approx \frac{LI^2}{T_{\text{ramp}}} \frac{L/R_{\text{sp}}}{T_{\text{ramp}}}$$

These losses represent only small corrections when $V^2/R_{\text{sp}} \ll P_{\text{rf}}$, or, using Eq. (29), when

$$\frac{T_{\text{ramp}}}{L/R_{\text{sp}}} \gg \frac{P_{\text{el}}}{P_{\text{rf}}}$$

For the reactor-grade example, $P_{\text{el}}/P_{\text{in}} \approx \frac{1}{3}$, $\eta \approx 0.7$, the above inequality requires that the ramp-up time be longer than about $\frac{1}{4}$ of the L/R_{sp} time. This restricts the temperature to somewhat less than 2 keV.

Restricting the temperature during a period of intense rf injection (perhaps 40 MW) requires a small heat confinement time during the start-up operation. In the above example, this may be as small as 30 msec. Poor confinement during the start-up phase may be helpful from the standpoint of runaway buildup, too. Even a small percentage ($\sim 1\%$) of reverse runaways²³ can seriously impede ramp-up if the runaways are well confined. If the runaways are poorly confined, then higher percentages may be tolerated, allowing higher ramp-up rates and, consequently, higher energy conversion efficiencies for a given density.

We are led thus to the following typical picture of rf ramp-up for pulsed tokamak operation. Start-up can proceed in a low-density plasma²⁴ where the rf power is also used to initiate the plasma. Density and rf power, and the ramp-up rate, are increased concomitantly as the plasma is brought to interesting densities 10^{13} – 10^{14} cm^{-3} . During this phase the temperature is purposefully kept low, possibly

through a deliberate degradation of the confinement of both runaway and thermal electrons. Hence the current is programmed to reach a large value prior to the density, and both reach large values prior to the temperature. The final step, in which the reactor is brought to reactor-grade temperature, occurs after the current is ramped up and as a result of ceasing the deliberate degradation of confinement.

VII. CONCLUSIONS

In this paper we have written down a set of circuit equations that describe the dynamics of an rf-driven plasma. In arriving at these circuit equations, we systematically introduce approximations with a goal of characterizing the driven plasma by a small number of functions of few variables that retain the essential physics. Greater accuracy, possible at the price of more complex circuit equations, may be obtained as a natural extension of the development here. The identification and calculation here of a minimal set of transport functions, however, provided a suitable and manageable description for a large class of important problems.

The calculations of the runaway function R and of the energy conversion function W_e , together pinpoint the preferred region for tokamak ramp-up operation. These functions depend only on the dimensionless parameter u . The separate contributions of runaway and stopped currents may be described using these functions of a single variable. The constitutive relations thus obtained are given by Eqs. (21). These equations are in a form both suitable for implementation in a transport code and amenable to obvious modification in the event that more complex runaway models are desired.

There are several caveats to bear in mind in using these formulas. First, the time scale for variation of the dc electric fields has been assumed long compared to other scales of interest, such as the particle deceleration times. A violation of this scale separation would affect the normalizations through v_r . Second, knowledge of the rf spectrum is unlikely to be complete. This knowledge is necessary to give S , the rf-induced flux. Even if the incident rf energy is followed by ray-tracing codes, it remains possible that other waves may be present. These other waves might arise either because of asymmetries in the particle distribution functions or nonlinear effects associated with the incident spectrum. Third, particle transport across field lines was neglected in comparison to the effects along field lines. The neglect of these effects is possible for stopped electrons if they are stopped before they reach a flux surface with significantly different conditions (v_r different). For runaway electrons, these effects are always important in that they provide a model for the runaway loss. As discussed after Eqs. (21), such a model may be included through a natural modification of Eq. (21c). In the absence of one particularly compelling model, at present, for runaway loss we have left the modification of Eq. (21c) as an open issue.

Finally, we should note that some of the most powerful conclusions of this paper occur in certain special cases. It is often the case that the rf spectrum is not only known, but also localized, which enables a particularly simple evaluation of the conversion efficiency, as in Eqs. (27). In the event

of moderate electric fields, or spectra localized at moderate phase velocities, it may be that $R = 0$ (no runaway production), and an accurate runaway loss model would not be needed. In the event that runaways are confined well, the spectrum must be chosen carefully to assure that $R = 0$.

ACKNOWLEDGMENTS

This work was supported by the United States Department of Energy under Contract No. DE-AC02-76-CHO-3073.

APPENDIX A: LANGEVIN EQUATIONS

Here we show that the conditional probability distribution $g(\mathbf{u}, \tau; \mathbf{u}')$ for Eqs. (4) satisfies Eq. (3). The derivation follows those given in Refs. 18 and 25. Because the process described by Eqs. (4) is a Markoff process, g satisfies the Smolucowski equation,¹⁸

$$g(\mathbf{u}, \tau + \Delta\tau; \mathbf{u}') = \int d^3\mathbf{u}'' g(\mathbf{u}, \Delta\tau; \mathbf{u}'') g(\mathbf{u}'', \tau; \mathbf{u}'), \quad (\text{A1})$$

for all $\tau > 0$ and $\Delta\tau > 0$. Let us define

$$r(\mathbf{w}, \mathbf{u}, \Delta\tau) \equiv g(\mathbf{u} + \mathbf{w}, \Delta\tau; \mathbf{u}).$$

Subtracting $g(\mathbf{u}, \tau; \mathbf{u}')$ from Eq. (A1) gives

$$\begin{aligned} g(\mathbf{u}, \tau + \Delta\tau; \mathbf{u}') - g(\mathbf{u}, \tau; \mathbf{u}') \\ = \int d^3\mathbf{u}'' [r(\mathbf{u} - \mathbf{u}'', \Delta\tau)g(\mathbf{u}'', \tau; \mathbf{u}') \\ - r(\mathbf{u} - \mathbf{u}'', \mathbf{u}, \Delta\tau)g(\mathbf{u}, \tau; \mathbf{u}')] , \end{aligned} \quad (\text{A2})$$

where, because of the normalization condition for probabilities, the second term in the integral may be reduced to $g(\mathbf{u}, \tau; \mathbf{u}')$. If we change the variable of integration to $\mathbf{w} = \mathbf{u} - \mathbf{u}''$, the right-hand side of Eq. (A2) becomes

$$\int d^3\mathbf{w} [r(\mathbf{w}, \mathbf{u} - \mathbf{w}, \Delta\tau)g(\mathbf{u} - \mathbf{w}, \tau; \mathbf{u}') - r(\mathbf{w}, \mathbf{u}, \Delta\tau)g(\mathbf{u}, \tau; \mathbf{u}')] .$$

For small $\Delta\tau$, the function $r(\mathbf{w}, \mathbf{u}, \Delta\tau)$ is highly localized about $\mathbf{w} = 0$. We may therefore expand the first term in the integral, assuming that \mathbf{w} is much smaller than \mathbf{u} , to give

$$\begin{aligned} r(\mathbf{w}, \mathbf{u} - \mathbf{w}, \Delta\tau)g(\mathbf{u} - \mathbf{w}, \tau; \mathbf{u}') \\ \approx r(\mathbf{w}, \mathbf{u}, \Delta\tau)g(\mathbf{u}, \tau; \mathbf{u}') \\ - \mathbf{w} \cdot \frac{\partial}{\partial \mathbf{u}} r(\mathbf{w}, \mathbf{u}, \Delta\tau)g(\mathbf{u}, \tau; \mathbf{u}') \\ + \frac{1}{2} \mathbf{w}\mathbf{w} : \frac{\partial^2}{\partial \mathbf{u} \partial \mathbf{u}} r(\mathbf{w}, \mathbf{u}, \Delta\tau)g(\mathbf{u}, \tau; \mathbf{u}') . \end{aligned}$$

Using this approximation in Eq. (A2), integrating by parts, dividing by $\Delta\tau$, and taking the limit $\Delta\tau \rightarrow 0$, we find as the equation for $g(\mathbf{u}, \tau; \mathbf{u}')$,

$$\frac{\partial}{\partial \tau} g = \frac{\partial}{\partial \mathbf{u}} \cdot \mathbf{A}g + \frac{\partial^2}{\partial \mathbf{u} \partial \mathbf{u}} : \mathbf{B}g , \quad (\text{A3})$$

where

$$\mathbf{A}(\mathbf{u}) = \lim_{\Delta\tau \rightarrow 0} - \langle \Delta\mathbf{u} \rangle / \Delta\tau ,$$

$$\mathbf{B}(\mathbf{u}) = \lim_{\Delta\tau \rightarrow 0} \langle \Delta\mathbf{u}\Delta\mathbf{u} \rangle / 2\Delta\tau ,$$

and

$$\langle \Delta\mathbf{u} \rangle = \int \mathbf{w} r(\mathbf{w}, \mathbf{u}, \Delta\tau) d^3\mathbf{w} ,$$

$$\langle \Delta\mathbf{u}\Delta\mathbf{u} \rangle = \int \mathbf{w}\mathbf{w} r(\mathbf{w}, \mathbf{u}, \Delta\tau) d^3\mathbf{w} .$$

Thus $\langle \Delta\mathbf{u} \rangle$ is the average value of $\mathbf{u}(\tau + \Delta\tau) - \mathbf{u}(\tau)$ given that $\mathbf{u}(\tau) = \mathbf{u}$ (and similarly for $\langle \Delta\mathbf{u}\Delta\mathbf{u} \rangle$) assuming that $\Delta\tau$ is sufficiently small that \mathbf{u} does not change appreciably. We then obtain

TABLE I. Coefficients for approximation to $R(\mathbf{u}, \mu = 1)$.

Z	a_0	a_1	a_2	a_3	b_2	b_3
1	-3.680 63	4.239 13	-4.558 94	-0.397 55	-1.227 74	1.414 50
2	-4.976 36	-16.090 15	0.831 88	0.217 37	6.846 15	-0.986 49
5	-4.276 87	-4.336 29	0.303 38	0.056 97	3.213 15	-0.477 49
10	-4.945 97	-1.534 82	0.101 12	0.030 87	2.452 88	-0.368 96

TABLE II. Coefficients for approximation to $W_i(\mathbf{u}, \mu = 1)$.

Z	a_2	a_3	a_4	b_1	b_2	b_3
1	0.166 12	-0.014 95	0.007 75	0.371 36	0.022 40	0.016 45
2	0.142 00	-0.040 48	0.011 45	0.122 53	0.003 84	0.024 40
5	0.098 80	-0.051 52	0.011 13	-0.194 84	0.005 59	0.023 62
10	0.065 37	-0.038 95	0.007 38	-0.324 56	0.027 97	0.015 26

TABLE III. Coefficients for approximation to $W_s(u, \mu = -1)$.

Z	a_2	a_3	a_4	a_5
1	-0.164 83	-0.134 20	0.153 46	-0.243 14
2	-0.141 86	-0.092 97	0.066 61	-0.128 70
5	-0.099 75	-0.047 81	0.006 06	-0.035 45
10	-0.066 51	-0.027 97	-0.002 47	-0.009 34

$$\begin{aligned} \langle \Delta u \rangle &= - \int_{\tau}^{\tau + \Delta\tau} \left\langle \frac{1}{u(\tau')^2} + \mu(\tau') \right\rangle d\tau' \\ &\approx - (1/u^2 + \mu) \Delta\tau, \\ \langle \Delta\mu \rangle &= \int_{\tau}^{\tau + \Delta\tau} \left\langle A(\tau') - \frac{1 - \mu(\tau')^2}{u(\tau')} \right\rangle d\tau' \\ &\approx - \left(\frac{1 + Z}{u^3} \mu + \frac{1 - \mu^2}{u} \right) \Delta\tau, \\ \langle \Delta\mu \Delta\mu \rangle &= \int_{\tau}^{\tau + \Delta\tau} \int_{\tau}^{\tau + \Delta\tau} \langle A(\tau') A(\tau'') \rangle d\tau' d\tau'' + O(\Delta\tau^2) \\ &\approx [(1 + Z)/u^3] (1 - \mu^2) \Delta\tau, \\ \langle \Delta u \Delta u \rangle &= \langle \Delta u \Delta\mu \rangle = \langle \Delta\mu \Delta u \rangle = O(\Delta\tau^2). \end{aligned}$$

Here we have made use of the properties of A given in Eqs. (5). Writing Eq. (A3) in spherical coordinates and substituting for the nonzero components of A and B , we obtain

$$\begin{aligned} \frac{\partial}{\partial\tau} g &= \frac{1}{u^2} \frac{\partial}{\partial u} u^2 A_u g + \frac{\partial}{\partial\mu} A_\mu g + \frac{\partial^2}{\partial\mu^2} B_{\mu\mu} g \\ &= \frac{\partial}{\partial u_{||}} g + \frac{1}{u^2} \frac{\partial}{\partial u} g + \frac{1 + Z}{2u^3} \frac{\partial}{\partial\mu} (1 - \mu^2) \frac{\partial}{\partial\mu} g. \end{aligned} \tag{A4}$$

This is the same equation as Eq. (3). Furthermore, from the definition g as a conditional probability, the initial condition for Eq. (A4) is also the same as for Eq. (3), namely, $g(u, \tau; u') = \delta(u - u')$.

APPENDIX B: NUMERICAL FITS

In this Appendix we give approximations for some of the important functions we have calculated. These are suitable for incorporating into modeling codes. The approximations were found by choosing a suitable analytic form containing several undetermined coefficients and adjusting those coefficients in order to minimize the maximum relative error. The technique for carrying out this procedure is described in Hastings' classic work.²⁶ The fits were made to the numerical data presented in Sec. IV. These data contain er-

rors because of the numerical methods used. The main source of error is because of the finite size of the numerical mesh and it is estimated that this introduces errors on the order of a percent. However, near $u = 0$, the relative error in the numerical data for W_s and its derivative becomes large because $W_s = O(u^4)$. Thus for $u < 0.5$, the fits were made using the following analytical approximation instead of the numerical data:

$$\begin{aligned} W_s &= \frac{\mu u^4}{Z + 5} \frac{(2 + Z + 3\mu^2)u^6}{3(3 + Z)(5 + Z)} \\ &+ \frac{2[(24 + 19Z + 3Z^2)\mu + (9 + Z)\mu^3]u^8}{(3 + Z)(5 + Z)(7 + 3Z)(9 + Z)} \\ &- [1041 + 1864Z + 1189Z^2 + 316Z^3 + 30Z^4 \\ &+ 10(417 + 497Z + 181Z^2 + 21Z^3)\mu^2 \\ &+ 5(9 + Z)(13 + 3Z)\mu^4]u^{10}/[5(2 + Z)(3 + Z) \\ &\times (5 + Z)(7 + 3Z)(9 + Z)(13 + 3Z)]. \end{aligned}$$

This result was obtained by solving Eq. (12) for small u using MACSYMA.²⁷ (The first two terms in this expansion are those derived by Fisch.¹⁴)

For each of the functions approximated, we give the analytic form of the approximation, the range in which it is valid, a table of coefficients, and the maximum relative error. The approximations should not be used outside the range given. Also, note that the relative error quoted is the error in fitting the approximation to the numerical data, which are in error by about a percent.

For $\mu = 1$ and $1.4 < u < 8$, the runaway probability R is approximated by

$$R(u, \mu = 1) = \exp\left(\frac{\sum_{i=0}^3 a_i (u - 1)^i}{\sum_{i=1}^3 b_i (u - 1)^i}\right),$$

where $b_1 = 1$ and the other coefficients a_i and b_i are given in Table I. The maximum relative error is 1%. For $\mu = 1$ and $1 < u < 1.4$, the same approximation may be used with small absolute error but large relative error. For $u < 1$ and all μ we have $R = 0$ identically.

For $\mu = 1$ and $0 < u < 5$, the energy imparted to the electric field W_s by stopped electrons is approximated by

$$W_s(u, \mu = 1) = \frac{\sum_{i=2}^4 a_i u^{2i}}{\sum_{i=0}^3 b_i u^{2i}},$$

where $b_0 = 1$ and the other coefficients a_i and b_i are given in Table II. The maximum relative error is 2%. For $\mu = -1$ and $0 < u < 1$, W_s is approximated by

$$W_s(u, \mu = -1) = \sum_{i=2}^5 a_i u^{2i},$$

TABLE IV. Coefficients for approximation to $(\partial W_s / \partial u) / u$ for $\mu = 1$.

Z	a_1	a_2	a_3	b_1	b_2	b_3
1	0.664 45	-0.360 32	0.073 28	0.177 69	-0.254 52	0.072 78
2	0.567 60	-0.389 84	0.086 34	-0.040 19	-0.246 73	0.085 08
5	0.399 06	-0.328 79	0.076 70	-0.282 81	-0.162 75	0.074 36
10	0.270 28	-0.232 61	0.052 72	-0.391 40	-0.075 26	0.049 81

TABLE V. Coefficients for approximation to $(\partial W_s/\partial u)/u$ for $\mu = -1$.

Z	a_1	a_2	a_3	a_4
1	-0.636 73	-1.399 60	3.376 62	-4.236 84
2	-0.557 77	-0.807 63	1.431 44	-2.038 66
5	-0.397 04	-0.338 11	0.236 07	-0.510 11
10	-0.266 00	-0.173 42	0.018 96	-0.133 49

where the coefficients a_i are given in Table III and the maximum relative error is 1.5%.

For $\mu = 1$ and $0 < u < 5$, the function $(\partial W_s/\partial u)/u$ is approximated by

$$\frac{1}{u} \frac{\partial}{\partial u} W_s(u, \mu = 1) = \frac{\sum_{i=1}^3 a_i u^{2i}}{\sum_{i=0}^3 b_i u^{2i}},$$

where $b_0 = 1$ and the other coefficients a_i and b_i are given in Table IV. The maximum relative error is 5%. For $\mu = -1$ and $0 < u < 1$, $(\partial W_s/\partial u)/u$ is approximated by

$$\frac{1}{u} \frac{\partial}{\partial u} W_s(u, \mu = -1) = \sum_{i=1}^4 a_i u^{2i},$$

where the coefficients a_i are given in Table V and the maximum relative error is 3%.

¹N. J. Fisch, Phys. Rev. Lett. **41**, 873 (1978).

²N. J. Fisch and C. F. F. Karney, Phys. Rev. Lett. **54**, 897 (1985).

³C. F. F. Karney, N. J. Fisch, and F. C. Jobses, Phys. Rev. A **32**, 2554 (1985).

⁴F. C. Jobses, S. Bernabei, T. K. Chu, W. M. Hooke, E. B. Meservey, R. W. Motley, J. E. Stevens, and S. E. von Goeler, Phys. Rev. Lett. **55**, 1295 (1985).

⁵N. J. Fisch, Phys. Fluids **29**, 172 (1986).

⁶R. W. Harvey, J. C. Riordan, J. L. Luxon, and K. D. Marx, in the *Proceedings of the 4th Topical Conference on Radio Frequency Plasma Heating*, Austin, Texas, 1981 (University of Texas at Austin, Austin, TX, 1981).

⁷C. S. Liu, Z. G. An, D. A. Boyd, Y. C. Lee, L. Muschietti, K. Appert, and J. Vaclavik, Comments Plasma Phys. Controlled Fusion **7**, 21 (1982).

⁸L. Muschietti, J. Vaclavik, and K. Appert, Plasma Phys. **24**, 987 (1982).

⁹Z. G. An, C. S. Liu, Y. C. Lee, D. A. Boyd, L. Muschietti, K. Appert, and J. Vaclavik, Phys. Fluids **25**, 997 (1982); **26**, 345 (1983).

¹⁰K. Appert, A. H. Kritiz, S. Succi, and J. Vaclavik, in the *Proceedings of the 11th European Conference on Controlled Fusion and Plasma Physics*, Aachen, 1983 (European Physical Society, Petit Lancy, Switzerland, 1983), Vol. 7D, p. 329.

¹¹K. Borrass and A. Nocentini, Plasma Phys. Controlled Fusion **26**, 1299 (1984).

¹²C. S. Liu, V. S. Chan, and Y. C. Lee, submitted to Phys. Rev. Lett.

¹³D. F. H. Start, Plasma Phys. **25**, 793 (1983).

¹⁴N. J. Fisch, Phys. Fluids **28**, 245 (1985).

¹⁵C. F. F. Karney and N. J. Fisch, Phys. Fluids **28**, 116 (1985).

¹⁶H. Dreicer, Phys. Rev. **117**, 329 (1960).

¹⁷C. F. F. Karney and N. J. Fisch, Phys. Fluids **22**, 1817 (1979).

¹⁸M. C. Wang and G. E. Uhlenbeck, Rev. Mod. Phys. **17**, 323 (1945), in *Selected Papers on Noise and Stochastic Processes*, edited by N. Wax (Dover, New York, 1954).

¹⁹N. J. Fisch and A. H. Boozer, Phys. Rev. Lett. **45**, 720 (1980).

²⁰T. M. Antonsen and K. R. Chu, Phys. Fluids **25**, 1295 (1982).

²¹M. Taguchi, J. Phys. Soc. Jpn. **52**, 2035 (1983).

²²L. Spitzer and R. Härm, Phys. Rev. **89**, 977 (1953).

²³D. C. Eder and E. J. Valeo (private communication).

²⁴F. C. Jobses, J. Stevens, R. Bell, S. Bernabei, A. Cavállo, T. K. Chu, S. Cohen, B. Denne, P. Eftimion, E. Hinnov, W. Hooke, J. Hosea, E. Mazzucato, R. McWilliams, R. Motley, S. Suckewer, G. Taylor, J. Timberlake, S. von Goeler, and R. Wilson, Phys. Rev. Lett. **52**, 1005 (1984).

²⁵E. M. Lifshitz and L. P. Pitaevskii, *Physical Kinetics* (Pergamon, Oxford, 1981).

²⁶C. Hastings, *Approximations for Digital Computers* (Princeton U. P., Princeton, 1955).

²⁷R. H. Rand, *Computer Algebra in Applied Mathematics: An Introduction to MACSYMA* (Pitman, London, 1984).